J. Membrane Biol. 52, 37–50 (1980)

The Journal of
Membrane Biology

Development of a New Coulter Counter System: Measurement of the Volume, Internal Conductivity, and Dielectric Breakdown Voltage of a Single Guard Cell Protoplast of *Vicia faba*

U. Zimmermann, M. Groves, H. Schnabl*, and G. Pilwat
Institute of Biophysical Chemistry, Nuclear Research Center, Jülich, West Germany

Summary. A new Coulter Counter is described which measures on single microscopic cells the volume, membrane breakdown voltage, and the underestimation of volume after breakdown, this last parameter reflecting in part the internal conductivity of the cells. The system requires very few cells for measurement and does not require the population to be normally distributed in volume or free of debris from the preparation of the cells.

The new development is to apply a voltage ramp across a Coulter orifice through which a particle flows. A differential dual orifice system is used to reduce the magnitude of the amplified ramp signal to that of the signal produced by the particle in the presence of a DC voltage across the orifice. Breakdown is detected by an underestimation of the cell volume once a critical voltage across the cell membrane has been established.

Measurements made on protoplasts isolated from guard cells of *Vicia faba* with a mean volume of 1800 μm^3 reveal a breakdown voltage of 1 V and an average volume underestimation of about 30% after breakdown. Variations in this underestimation reflect the different internal structure of the protoplasts in terms of the size and number of nonconducting compartments. Different stages of vacuole development exist in each preparation. The breakdown voltage of 1 V suggests that only one membrane breaks down and that the electromechanical properties of these protoplast membranes are similar to other cell systems, when the pulse length dependence of the breakdown voltage is taken into consideration.

The electro-mechanical properties of plant membranes may play a key role in the transduction of pressure signals into changes of the intrinsic electric field and ion transport of the membrane, this being very important for both osmoregulation and plant growth [5, 7, 34, 35, 36, 39]. At present, the only method capable of providing insight into the electromechanical properties of cell membranes is that of dielectric breakdown [43]. The dielectric breakdown voltage of the membrane is determined by measuring the size distribution of a cell suspension with increasing field strengths in the orifice of a hydrodynamically focusing Coulter Counter [38, 43]. Breakdown is detected by an underestimation of the cell size beyond a critical field strength, the membrane of the cell temporarily becoming highly conducting so that current flows through the cell interior. Thus the degree of cell size underestimation reflects the relationship between the internal conductivity of the cell and the external conductivity [17, 43].

Such a measurement requires the size distribution to be approximately normal and uses at least 10^5 cells per distribution to achieve sufficient accuracy. At each field strength setting a complete distribution is measured requiring something like 10^6 cells altogether. Unfortunately, many cell suspensions are not normally distributed and are in relatively low yield, in particular the protoplasts used here which are prepared by enzymatic degradation from tissue cells [33] and suffer from considerable contamination arising from cell and tissue debris. The conditions therefore severely limit the use of the Coulter Counter for such measurements. In addition, the time required (5–10 min) to perform a complete breakdown run using a Coulter Counter, precludes the study of either the kinetics of volume changes in response to osmotic stress, or the time-dependent influence of agents which alter the membrane structure and composition on the breakdown voltage [25].

In this communication, we describe a new technique for simultaneously measuring cell volume,

* *Present address:* Institute of Botany and Microbiology, Technical University, Munich, W. Germany.

0022-2631/80/0052-0037 $02.80

membrane breakdown voltage, and internal conductivity on individual cells, protoplasts, and vesicles. The system is a modification of the hydrodynamically focusing Coulter Counter. In contrast to the Coulter Counter, the voltage across the orifice is no longer held constant after the volume of a single particle has been determined. Instead, in conjunction with a specially designed detector system, a linear voltage increase is applied across the orifice sufficient to cause breakdown. Upon breakdown a change in the slope of the signal caused by the particle is observed.

For the purposes of this study stomata guard cell protoplasts from *Vicia faba* were used [29, 30] and the characteristic breakdown voltage, volume, and a parameter related to the cell internal conductivity were measured. The protoplasts used are of special interest because stomata play a vital role in the regulation of plant metabolism and water relations [8, 15, 21–23, 26–28, 31].

Principle of Operation

In the modified version of the Coulter Counter system presented here a single cell is subjected to an ever increasing electric field during its passage through the orifice. At the beginning of the orifice the cell is exposed to a low electric field enabling a measurement of its size to be made from the height of the particle signal. A voltage ramp is then applied across the orifice sufficient to induce breakdown of the membrane of the cell whilst it is still in the orifice. After breakdown has occurred, the current is then partly forced through the cell interior. The field induced change in membrane resistance beyond the critical field strength is detected by a decrease in the resistance of the orifice, hence a change in slope of the "ramp signal" occurs.

The concept described above requires substantial modification of the hydrodynamically focusing Coulter Counter system [38, 43]. A long transit time (~ 100 μsec) of the particle through the orifice is used to allow enough time for the voltage ramp application. In addition the electronics must have a high resolution to detect both the small signal induced by the particle passing the orifice and the large superimposed ramp signal that appears in response to the voltage ramp applied across the orifice. To this end a pair of matched orifices are mounted in parallel. There is a measuring orifice through which cells are sucked, and another, the reference orifice through which only particle-free electrolyte flows. The outputs from these are fed into a differential amplifier via current pre-amplifiers. Thus the ramp signal results from the subtraction of two similar ramp voltages from each other and is thereby markedly reduced in magnitude in comparison with the ramp voltage. The size of the ramp signal depends upon the mismatch between the two orifices caused by the presence of a particle in the measuring orifice.

Equipment Design

A schematic diagram of the germane idea is shown in Fig. 1, together with some of the electronics. As mentioned before, two orifices are connected in parallel via two independent current pre-amplifiers which are fed into the two sides of a differential amplifier. When the two inputs to this amplifier are matched to one another, that is the pre-amplifiers have the same gain, a voltage ramp applied to the two orifices would produce only a minor disturbance on the differential amplifier output. However, when a particle is present in the measuring orifice, a "ramp signal" appears at the output, its magnitude being proportional to the mismatch induced by the particle. A marked change in slope of the ramp signal then indicates breakdown of the cell, the change in slope being directly related to the internal conductivity of the cell [17, 38].

The actual orifices used come from the Metricell design [18] and display very reasonable hydrodynamic focusing even with the low flow velocity of 1 m/sec used in these experiments. The low speed is required to yield a 150 μsec transit time of the particle through a 50 by 150 μm long orifice. It is during this time interval that a sequence of logic events are carried out with the subsequent application of the voltage ramp when all logic conditions have been satisfied.

Figure 2 schematically shows the sequence of events that take place during an experiment, whilst Fig. 3 describes the associated electronics. Referring to Fig. 2, a cell arrives in the measuring orifice producing a trapezoidal shaped pulse when a DC voltage is applied across the orifice. If the leading edge of this pulse rises above the threshold of a trigger module (indicated in Fig. 2*b*), sizing of the cell is performed using a window discriminator, termed a pulse size discriminator (PSD) (Fig. 3). A suitable delay of about 30 μsec is introduced between the trigger and the PSD to ensure that the particle has had time to enter the central, axially uniform field region of the orifice – i.e., the PSD monitors a section of the plateau of the trapezoidal particle pulse. If the cell size corresponds to that preset by the PSD, a voltage ramp is then applied across the orifices. Data collection by an analog to digital converter (ADC) which is controlled by a triggerable external clock begins just prior to the commencement of the ramp.

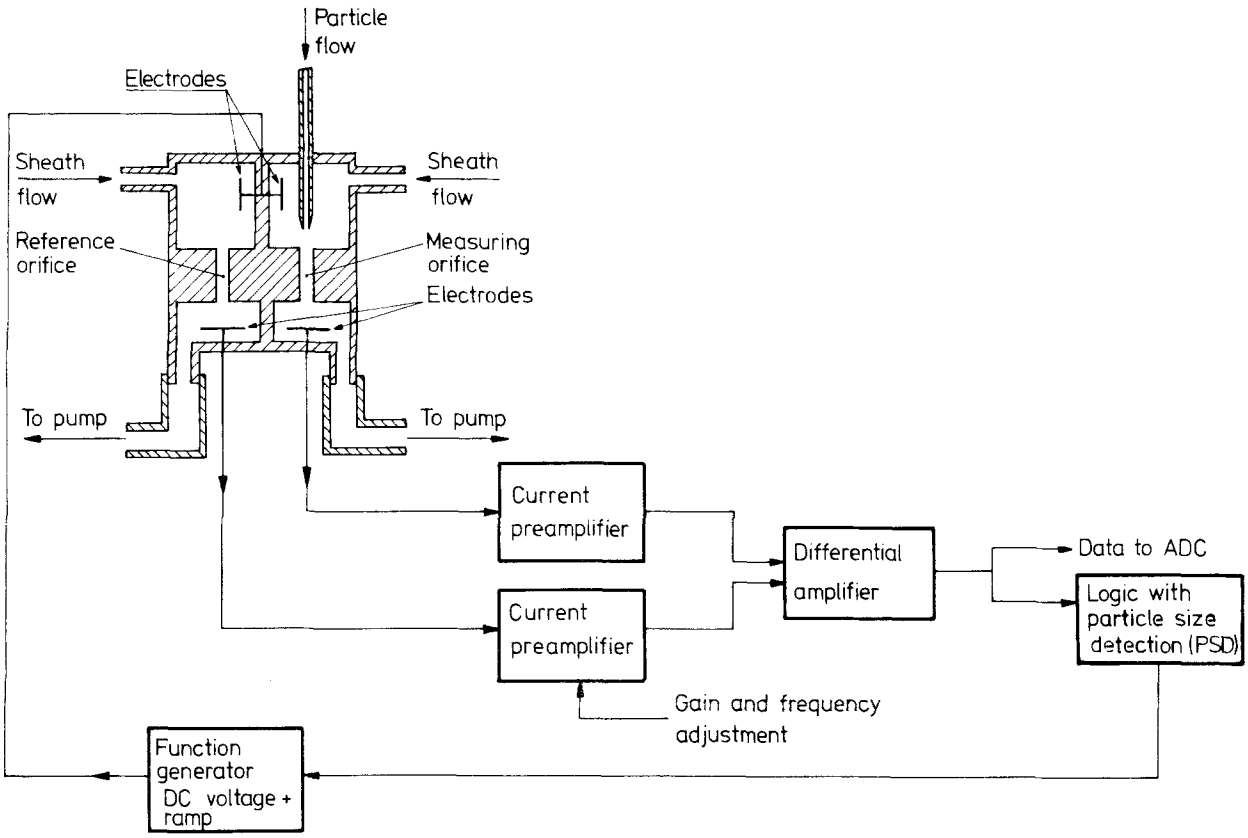

Fig. 1. Dual orifice system coupled to a differential amplifier. Two identical orifices through which electrolyte is sucked are connected in parallel via two independent current pre-amplifiers to the noninverting and inverting inputs of a differential amplifier. Particles flow only through the measuring orifice, producing from the differential amplifier a voltage pulse which is then detected and analyzed. The function generator supplies a voltage ramp across both orifices when a particle is detected. Consequently, the particle is exposed to an ever increasing field strength as it passes through the orifice. The differential amplifier then reduces the resulting ramp signal to a signal proportional to the mismatch between the orifices due to the particle presence. Breakdown causes a change in this mismatch and therefore a break in the linearity of the ramp signal

Once a single particle experiment has been performed, the whole equipment lies idle for 1100 μsec to allow both the electronics and the orifices to restabilize after termination of the ramp and the particle exit from the measuring orifice. A reference experiment is then triggered by a so-called "retrigger" module (*see* Fig. 3). For this experiment the same logic is used as for the real experiment (i.e., when a particle is present) only this time the PSD system is bypassed. The specially designed external clock takes advantage of the importance sampling capability of the ADC by not clocking it, and thereby not taking any data, during the idle period. The ADC is CAMAC interfaced to a minicomputer (PDP 11/40).

Consequently, as shown in Fig. 4, each run consists of two experiments, the first with a particle present and the second without. Subtraction of the latter from the former then removes any residual mismatching of the parallel orifice system. The problem of residual mismatching arises from differences in the temperature characteristics of the two orifices which cannot be removed by the differential amplifier system, thus the need for the reference experiment. Figure 4 demonstrates how well the subtraction process removes this residual mismatching effect when using Latex particles of 14 and 18.5 μm in diameter.

The residual mismatch shown on the right of Fig. 4*b* is due to small flow rate variations between the two orifices causing differential heating of them. This is exemplified by the use of a pair of non-matched thermistors (in place of the orifices) which display a resistance change of 4% per °C; similar signals to those seen in Fig. 4*b* are observed. On the other hand, if a pair of carbon resistors are substituted, the ramp is applied and the gain on the pre-amplifiers are matched, the output from the differential pre-amplifier remains zero. The effects of small

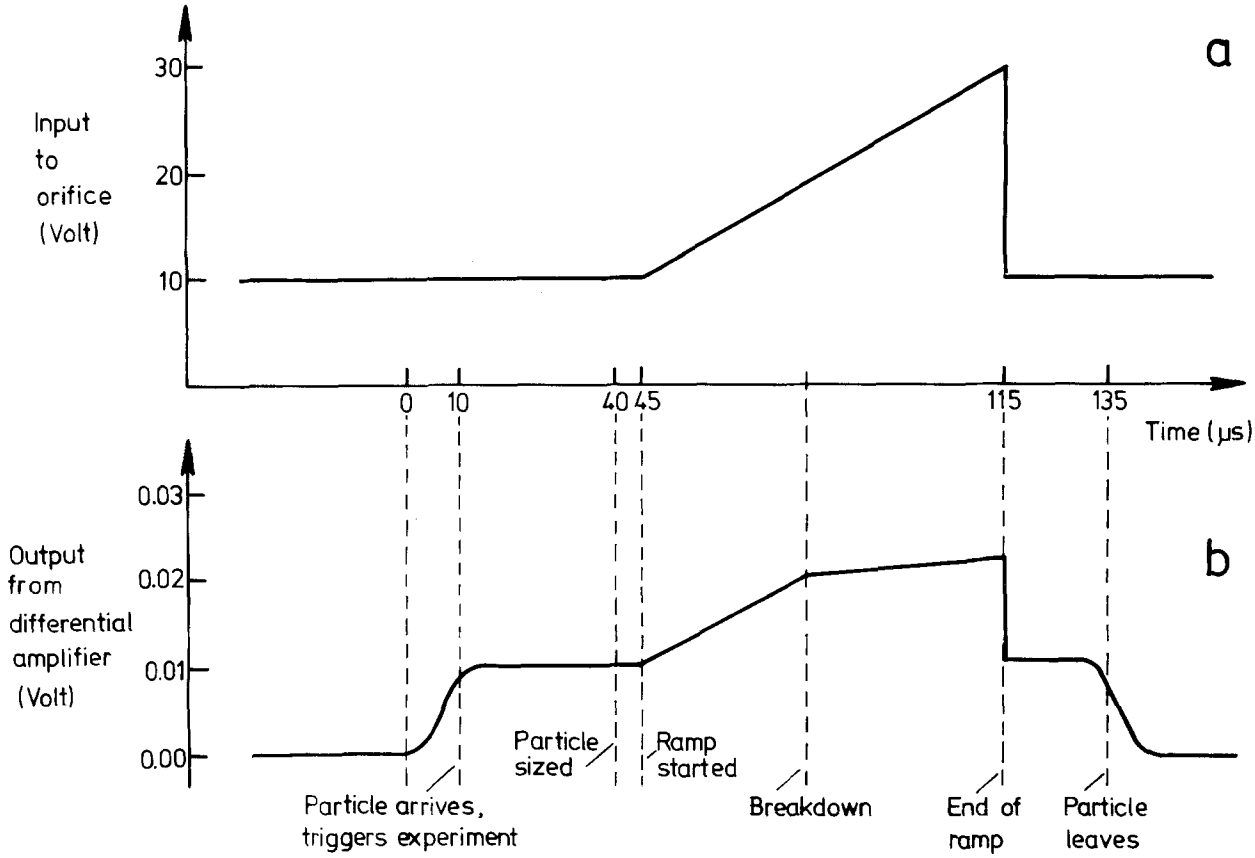

Fig. 2. Sequence of events upon the arrival of a particle in the measuring orifice. The output from the function generator is shown (*a*) together with an idealized output signal from the differential amplifier (*b*). Referring to *b*, particle arrival in the measuring orifice is detected by a trigger discriminator after which a delay is introduced before measuring the particle size. If the particle detected is within the desired size range, data collection commences and shortly afterwards the voltage ramp is applied (*a*). Breakdown is denoted by a change in the slope of the output from the differential amplifier. The ramp is subsequently terminated, leaving only the DC voltage (*a*), and the particle exits from the orifice (*b*)

temperature drifts of 0.02 to 1 °C between the two orifices can be removed by altering the pre-amplifier gains, and any frequency mismatch by a trim capacitor across the feedback resistor of one of the pre-amplifiers. In the reference experiment of Fig. 4*b* such adjustment has already been performed to minimize the disturbance of the differential amplifier output when a ramp is applied.

One way to measure the temperature increase in the orifice is to determine the degree of mismatch produced by the ramp voltage when one of the orifices is replaced by a carbon resistor of the same resistance. The carbon resistor shows virtually no temperature dependence, whilst the resistivity of a 0.1-M NaCl solution varies 2% per 1 °C. Thus, the degree of bending of the ramp signal will allow an estimate of the resistance change and, in turn, of the temperature change to be made. The degree of bending is measured by using the mismatch observed at the end of the ramp signal, relative to that at the beginning. Using a DC voltage of 10 V and a ramp of 20 V, a change of temperature of about 0.1 °C is observed[1]. The value of 0.1 °C is close to that ΔT, calculated from the heat capacity, C_p [g °C/J], the energy input, E [J], and the mass of fluid, M [g], in which the energy is dissipated, i.e., $\Delta T = C_p \cdot E/M$. For a 50×150 μm orifice with a resistance of 120 kΩ, the temperature increase is about 0.11 °C, assuming a particle transit time of 100 μsec during which a DC voltage of 10 V and a 70 μsec long 0.285 V/μsec ramp is applied. On the other hand, for the 60×60 μm orifice often used in breakdown measurements [38, 39, 42], the corre-

[1] The total effect of the DC voltage is not fully seen, as the current pre-amplifiers are so matched that at the beginning of the ramp no ramp signal appears. However, this does not affect the above calculation by much. The curvature of the ramp signal can be described by a square law dependence of signal *vs.* input voltage. This is in accordance with the statement that the curvature is due to a temperature dependence, as the energy input is proportional to the square of the applied voltage.

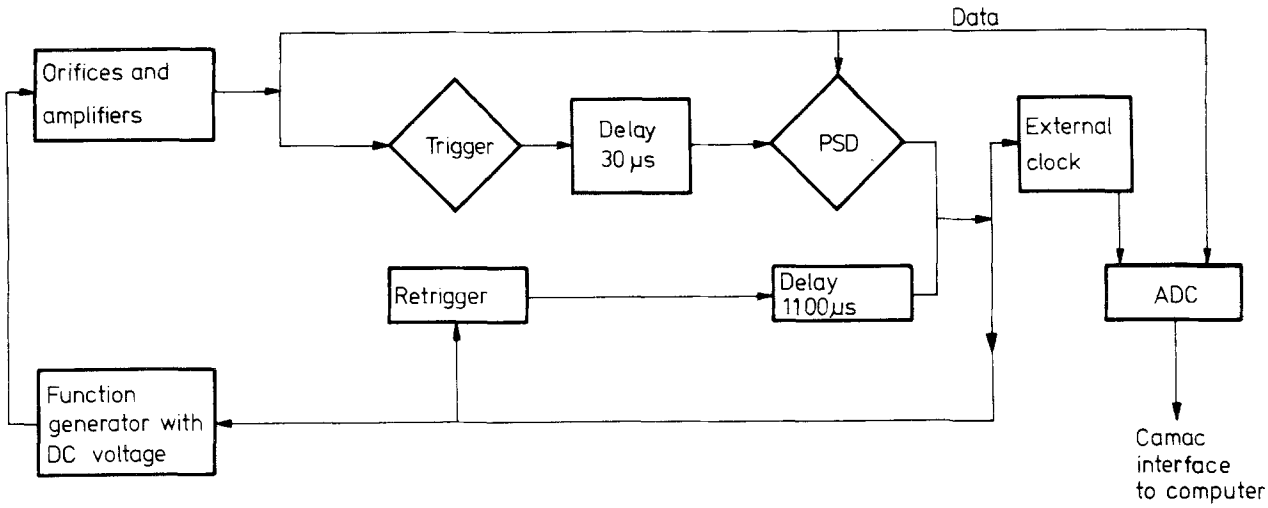

Fig. 3. Block diagram of electronics including logic functions. The output from the differential amplifier is fed into a trigger discriminator (Ortec 550) and also to a linear gate (Ortec 426) which is gated-on following a suitable delay (Ortec 416 A) of the trigger discriminator pulse. The pulse size discriminator (PSD) consists of the aforementioned linear gate together with a window discriminator (Ortec 550) and is used to discriminate against particles with undesirable sizes. The output pulse from the PSD starts the data collection and the voltage ramp (via the external clock and function generator, respectively) and triggers a retrigger module (*see* text for description). The above sequence of events is described in Fig. 2

sponding parameters are 20 V_{DC}, 20 kΩ resistance and a transit time of 10 µsec. Under these conditions a particle would experience a temperature increase of about 0.15 °C by the time it reached the maximum field region of the orifice. It can be concluded from the above that just as for the hydrodynamically focusing Coulter Counter, no substantial heating of the orifices occurs. Consequently, an effect of temperature increase upon the measured breakdown voltage can be excluded.

It will be noted from Fig. 4*b* that spikes appear both at the beginning and end of the ramp. These arise from the low common mode rejection ratio of the differential amplifier for frequencies in the 0.1 to 1 MHz range. Essentially, the first spike obscures the first 10 µsec of the ramp information.

Experimental Analysis

The cell volume can be estimated from two sections of the curve presented in Fig. 5. For the first estimation, the plateau region of the particle signal before ramp application yields the size as normally detected by the Coulter Counter. For nonconducting particles [16, 20] the relative change in orifice resistance, $\Delta R/R_0$, is equal to the particle size = shape factor × particle volume (fv_p) divided by the effective orifice volume, v_0,

$$\frac{\Delta R}{R_0}=\frac{fv_p}{v_0}$$

which can be rewritten in terms of the orifice current as

$$\frac{|\Delta I|}{I_0}=\frac{fv_p}{v_0} \tag{1}$$

where I_0 and $|\Delta I|$ are the orifice current and absolute change in orifice current, respectively.

As stated above, the electrical size measurement is equal to the particle's real geometric volume, v_p, times a shape factor term, f, which takes into account the additional field line disturbance due to particle shape [11]. The output (ΔV) from the current preamplifier is related to $|\Delta I|$ by $\Delta V=|\Delta I|R_F$, where R_F is the feedback resistor of the preamplifier, and the current I_0 can be rewritten as

$$I_0=\frac{V_{DC}}{R_0}$$

where V_{DC} is equal to the applied DC voltage minus the electrode polarization voltage. The polarization was measured in each experiment and varied between 0.5 and 1 V. Thus,

$$\frac{|\Delta I|}{I_0}=\frac{\Delta V}{R_F}\cdot\frac{R_0}{V_{DC}}=\frac{\Delta V}{V_{DC}}\cdot\frac{1}{G} \tag{2}$$

where G is the gain of the preamplifier.

Combining Eqs. (1) and (2) yields

$$v_p=\frac{1}{f}\cdot\frac{\Delta V}{V_{DC}}\cdot\frac{v_0}{G}. \tag{3}$$

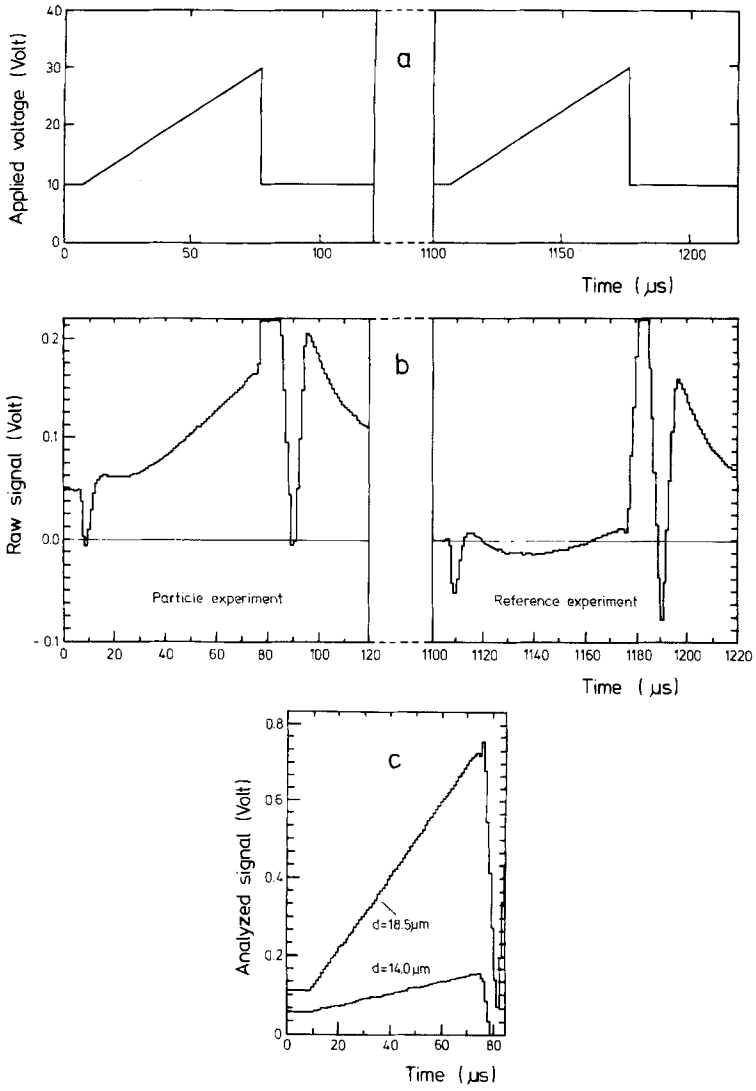

Fig. 4. An experimental run showing the raw (*b*, from the ADC) and analyzed signal (*c*, from the computer) when Latex particles are present, together with the applied voltages across the orifices (*a*). The two ramp applications are separated by 1.1 msec. The first of these is ellicited by a suitably sized particle (14 µm diameter Latex particle) in the measuring orifice, part of the plateau section of the particle pulse being shown in the first 5 µsec of (*b*) (the ADC is activated only after the PSD pulse). In the reference experiment the ramp is started by the retrigger module so that in this case the raw signal represents the degree of matching of the two orifice systems without the presence of a particle. Subtraction of the reference experiment from the real experiment (particle present) yields the analyzed signal (*c*). The ramp section of *c* reflects the mismatch between the orifices caused solely by the presence of a particle in the measuring orifice. For this measurement two particles of 14 and 18.5 µm diameter were used

An equivalent equation to (3) holds true for the second volume estimation, termed v_r, taken from the ramp signal before breakdown. Because this is a time derivative signal, the applied voltage must be expressed as such, i.e., dV/dt, thus

$$v_r = \frac{1}{f} \cdot \frac{\left(\frac{d\Delta V}{dt}\right)}{\left(\frac{dV}{dt}\right)} \cdot \frac{v_0}{G}. \tag{4}$$

It is obvious that the two volume calculations v_p and v_r should agree with each other for a given cell.

Fitting of the ramp signal by regression analysis using two straight lines yields an intersection point correlated with the membrane breakdown, if present. From the time, t, at which the ramp signal changes slope, the critical field in the orifice, E_c, is given by

$$E_c = \left(V_{DC} + \frac{dV}{dt} \cdot t\right) \Big/ L$$

where L is the effective orifice length, $L = 1.64r + l$ [12]. The terms r and l are the orifice radius and length, respectively. The critical membrane potential, V_c, immediately below breakdown, that is whilst the cell is still ideally nonconducting, can be calculated by solving the Laplace equation as applied to the system of orifice, electrodes and cell [17, 38]:

$$V_c = faE_c \tag{5}$$

where a is the radius of the spherical cell and f has the value 1.5 for spherical cells. Equation (5) is derived for a particle of spherical shape with a homogeneously conducting interior surrounded by a nonconducting membrane. As pointed out previously [40, *see also*

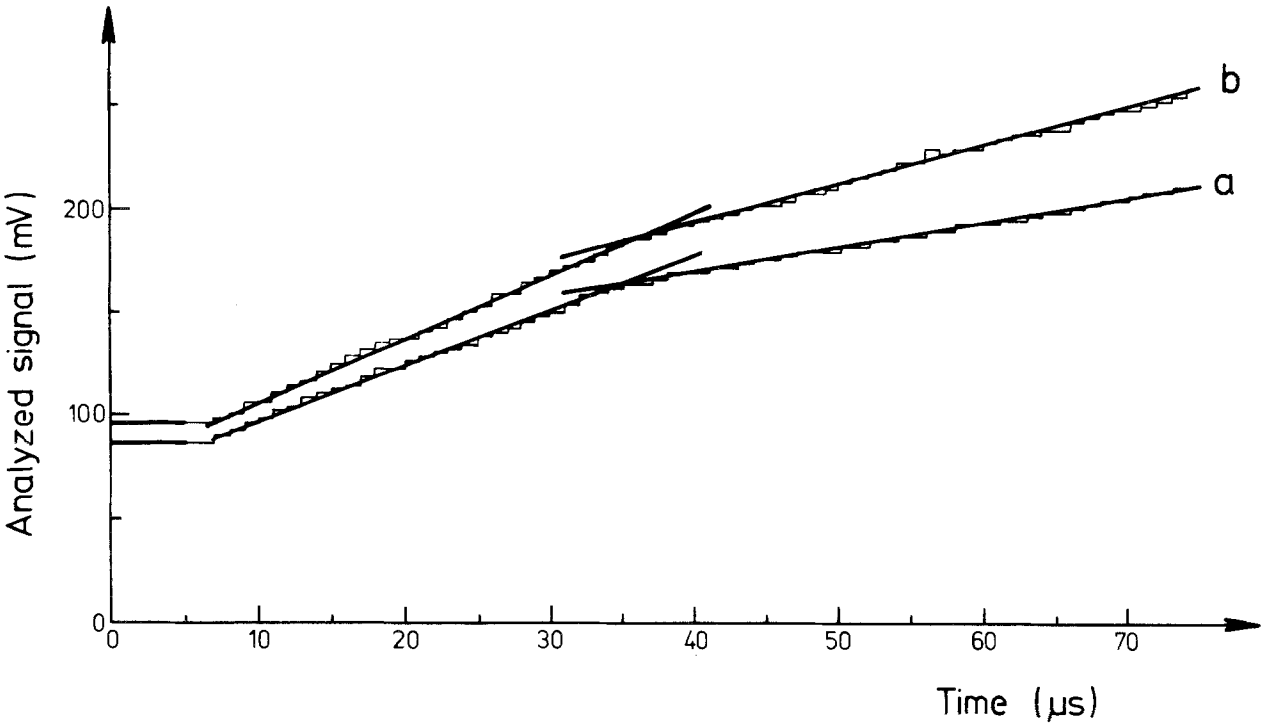

Fig. 5. Analyzed data from two protoplasts of stomatal guard cells of *Vicia faba* of different volumes displaying different changes in ramp slope after breakdown. The protoplasts were incubated at 20 °C in 600 mM mannitol with 80 mM Tris and 1 mM $CaCl_2$ at pH 6.5 10 min prior to the experiment. Shown is the pulse height after particle sizing (*see* Fig. 2) and then the ramp signal showing breakdown. The volume of the cell is first calculated from the pulse height of the plateau region (first 5 μsec of the signal) and then from the slope of the ramp signal before breakdown (*see* text). The critical membrane potential, V_c, at which breakdown occurs, is obtained from the orifice voltage at which the change of slope appears. The relative change in slope, R_s, is described by the ratio of the slope after breakdown to that before. From signal (*a*) the two volume calculations (v_p, v_r) yielded 1512 μm^3 and 1508 μm^3, respectively. The critical membrane potential, V_c, was 0.98 V, and the ratio of slopes, R_s, was 0.47 (correlation coefficient = 0.999). Signal (*b*) represents a cell with $v_p = 1740\ \mu m^3$, $v_r = 1749\ \mu m^3$, $V_c = 1.02$ V, and $R_s = 0.65$ (correlation coefficient = 0.997). For the calculation of the volume and of the critical membrane potential, a gain of $G = 1.47$ and a polarization voltage of 0.5 V were taken into consideration

2, 3, 4, 32] it is quite conceivable that the breakdown voltage is overestimated by using Eq. (5) due to time-dependent relaxation and polarization processes within the membrane. On the other hand, recent experiments on *Valonia utricularis* cells using the charge pulse technique [2] have shown that, at least for *Valonia* cells, the overestimation, if any, is very small. The relative size of the cell after breakdown, R_s, is given as the ratio of the slopes of the ramp signal after to before breakdown. Finally, it should also be noted that the equation preceding Eq. (1) is only valid up to an upper frequency limit when the capacitance reactance of the membrane becomes comparable to the access impedance $R(\rho_i + 0.5\,\rho_a)$ with R radius, ρ_i and ρ_a internal and external resistivities. The precise relationship for the time constant is

$$T = RC_m \frac{\rho_i + 0.5\,\rho_a}{1 + RG_m(\rho_i + 0.5\,\rho_a)}$$

which includes consideration of both membrane capacitance C_m and conductance G_m per unit area. This was discussed extensively by Schwan [32]. The question may arise as to whether the Fourier content of the ramp spectrum is well below the relaxation frequency. This is probably the case, although the theoretical estimates are different due to the lack of data. However, measuring tumor cells BT3C by means of the new Coulter Counter system and comparing these data with those obtained by measurements with the hydrodynamically focusing Coulter Counter (*unpublished results*), identical results were found even though the passage time of the particle within the orifice of the Coulter Counter, AEG-Telefunken, is higher by a factor of 100.

Materials and Methods

Plant Material

Seed of *Vicia faba* L. (cv. grünkernige Hangdown) were germinated and grown in peat moss in a growth chamber at 22 ± 1 °C (day)

[2] Zimmermann, U., Benz, R. 1979. Dependence of the electrical breakdown on the charging time in *Valonia utricularis*. *J. Membrane Biol.* (*in press*).

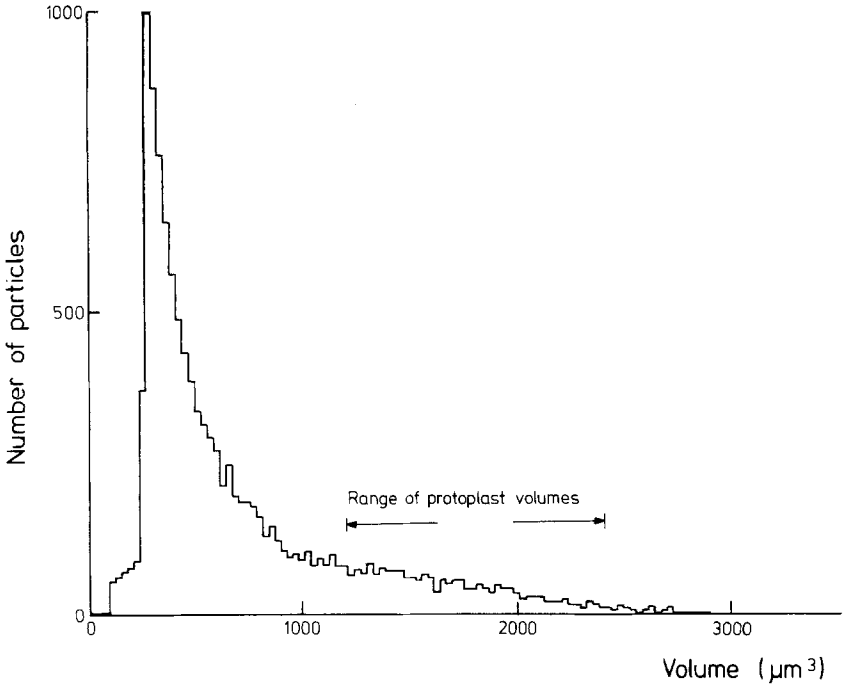

Fig. 6. Distribution of protoplasts of stomatal guard cells of *Vicia faba* and cell debris measured by a hydrodynamically focusing Coulter Counter using a 60 μm diameter orifice. The arrows indicate the range of protoplast volumes from a typical preparation. The rest of the particles represent extraneous matter such as cell debris

and 17±1 °C (night) with a 12 hr light period (15,000 Lx). The plants were watered three times a week with tap water. Unless otherwise stated, the plants used for preparation were grown in the months of September to December, 1978.

Epidermal Peels

The 2nd to 4th fully extended leaves of 3-week-old *Vicia* plants were cut just before commencement of the light period and placed in distilled water. Strips of epidermis (abaxial) were peeled, floated in 0.23 M mannitol, and brushed gently with a dissecting needle to remove adhering mesophyll cells.

Isolation of Guard Cell Protoplasts

The isolation procedure of guard cell protoplasts of *Vicia faba* has already been described [29, 30]. However, some conditions were modified for the current investigation. An incubation of 60 min (T=30 °C) in a mannitol solution (0.23 M; $CaCl_2$ 1 mM; cellulysin 4% wt/vol, Calbiochem, pH 5.6) was required for the lysis of the epidermal and mesophyll cell walls. After removing the epidermal and mesophyll cell protoplasts by centrifuging (300×g, 10 min) the epidermal strips with the intact guard cells were washed out with a mannitol solution (0.4 M; $CaCl_2$ 1 mM) and were incubated for 2 hr in a medium containing cellulysin (4% wt/vol; mannitol 0.4 M; $CaCl_2$ 1 mM; pH 5.6) at 30 °C whilst gently shaking. The concentration of mannitol was increased from 0.4 to 0.5 M (incubation time being 1.5 hr) and finally to 0.6 M (incubation time 2.5 hr). After centrifuging (300×g, 10 min), the released guard cell protoplasts were washed out with 0.6 M mannitol ($CaCl_2$ 1 mM) and filtered once through a sieve (mesh 25 μm). This procedure was followed by a second centrifugation step (300×g, 5 min). The concentrated suspension of the guard cell protoplasts was stored at 4 °C and used within the next 6 hr. Unless otherwise stated, just prior to the experiment the protoplasts were allowed to equilibrate to 20 °C in a solution of 600 mM mannitol plus 80 mM Tris and 1 mM $CaCl_2$ at pH 6.5. This provided the right conductivity of solution to match the identical sheath flow solution of the orifice system.

Protoplast Shape under Flow

In addition to monitoring the size of the protoplasts as observed under a light microscope, their shape was monitored in a flow chamber similar to that used in the experiments described in this paper (G. Pilwat & U. Zimmermann, *unpublished results*). The protoplasts remained spherical throughout, thus a shape factor, f, of 1.5 was used in the analysis. The shape factor of 1.5 assumes that the radius of the capillary is infinite compared with the cell radius. It should be noted that in the device described here the ratio of the radius of the cells to that of the orifice is about 0.3. According to Gregg and Steidley, the overestimation of the volume is only 4% and therefore within the error of the measurement [10].

Results

Protoplasts isolated from the stomatal guard cells of *Vicia faba* were sucked through the measuring orifice at a rate of 20 cells/sec. The PSD was adjusted so that only cells of a volume range 1200 to 2400 μm^3 were monitored. This volume range corresponds with that measured under a light microscope (mean volume 1600 to 2000 μm^3) depending on the preparation, the physiological state of the plants, and the external osmolarity. A volume distribution, as detected by a hydrodynamically focusing Coulter Counter normally used for breakdown measurements, is shown in Fig. 6.

Table 1. Averaged values of breakdown measurements on individual protoplasts of stomatal guard cells isolated from *Vicia faba*

Expt. No.	Volume calculated from the pulse height, v_p (μm^3)	Volume calculated from the ramp signal, v_r (μm^3)	Membrane breakdown voltage, V_c (V)	Ratio of ramp signal slope after breakdown to that before, R_s	Number of protoplasts
1	1880 ± 80	1910 ± 150	1.02 ± 0.11	0.62 ± 0.17	77
2	1720 ± 110	1730 ± 130	0.98 ± 0.05	0.73 ± 0.08	45
3	1280 ± 180	1330 ± 190	0.95 ± 0.08	0.72 ± 0.09	56

[a] The experiments were made on separate days with fresh protoplast preparations.

From the dependence of such a distribution upon electric field strengths through the orifice, it would obviously be impossible to draw conclusions regarding breakdown. The actual protoplasts are buried in the region indicated in Fig. 6, the rest of the distribution being made up of debris of cell remnants, including chloroplasts that have clumped together.

In contrast to the problems presented by the normal hydrodynamically focusing Coulter Counter, breakdown on single cells can readily be detected by the new equipment described here. Figure 5 comprises two runs made on individual protoplasts, one in which the degree of underestimation, $1-R_S$, equals 53% (*a*), and the other with $1-R_S$ equal to 35% (*b*). The analyzed signals are shown overlayed with the two intersecting straight lines fitted by regression analysis. The zero time for the fitting of the ramp before breakdown is taken as 3 μsec after the commencement of the ramp, there being a 2 μsec delay time before the ramp is established properly.

Table 1 lists the averaged values of volumes, breakdown voltages, and relative sizes after breakdown, R_S, for many of such experiments made on separate days with fresh protoplast preparations. The breakdown voltage is of the order of 1 V and the average degree of underestimation is 30 to 40%. The lack of correlation between the breakdown voltage and cell volume agrees well with other findings on erythrocytes [39, 42].

In analyzing the data, certain criteria were applied regarding the signal shape. Firstly, the two volume measurements, v_p and v_r, must be within 15% of each other. The error here allows for small variations in the polarization voltage as well as the fact that v_r is far more sensitive to the intrinsic particle shape than v_p which leads to a greater error in v_r (e.g., a 1° slope on the particle pulse shape will lead to a change in v_r of 5%, but of only 0.1% for v_p). Secondly, the value R_S, which yields a direct measure of the cell underestimation after breakdown, should be less than 0.85 in order to justify the assignment "breakdown". The ratio of the number of cells showing breakdown to the total number of cells measured with a good correlation between v_p and v_r was 80%. The remaining 20% reflect the presence of debris particles as seen from Fig. 6.

Such measurements as presented here require that a careful check of the system should be made to be certain that the results reflect real cell parameters and not artifacts generated by the measuring system. To this end, the following experiments were performed.

As Latex particles do not show breakdown [39, 43] and are nonconducting spheres, they are ideal test particles. Consequently, Latex particles of various diameters were subjected to the same experimental procedure as the protoplasts. The excellent "ideal" response from such a particle has already been presented in Fig. 4*c*. Very small differences (< 10%) between the volume estimations, v_p and v_r, were observed in most cases, and the underestimation parameter, R_S, used to indicate breakdown on biological cells rarely varied below 0.9 and in general ranged from 0.9 to 1.1, suggesting only random variation. This variation would arise from small irregularities in the pulse shape as detected without ramp application. The range of Latex particle volumes for which the equipment has so far been shown to satisfactorily work was 1000 to 3500 μm^3, corresponding to diameters of 12.4 to 18.8 μm, respectively.

The same "ideal" results as referred to above were also observed if pulses of Latex particles obtained without voltage ramp application, were multiplied with a ramp function of appropriate magnitude within the computer. In a few cases, the volume estimations v_r and v_p did not correlate well with each other, this being due to a poor plateau region of the particle shape. If the same experiment was now performed with protoplasts instead, a test of whether or not the fluctuations in the pulse shape may account for the observed breakdown could then be made. The same results as observed with Latex particles were obtained. Thus the breakdown seen in protoplasts cannot be attributed to irregularities in the cell passage through the orifice and hence in the pulse shape. Out of 81 such experiments, only 3 showed the kind

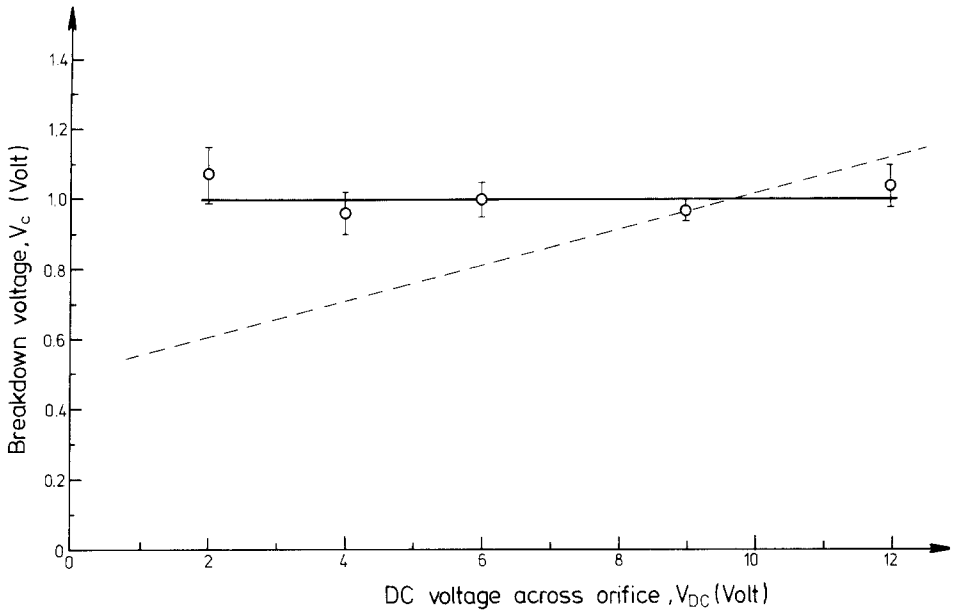

Fig. 7. Breakdown voltage of protoplasts measured with different initial DC voltages across the orifice. The dashed line was calculated assuming that the break in the ramp signal is a system artifact and thereby appears at a constant time after the beginning of the ramp corresponding to a voltage, V_{art}, no matter what DC voltage (V_{DC}) is applied. Consequently, any change in V_{DC} would induce an apparent variation in V_c (calculated from the orifice voltage, $V_{DC} + V_{art}$). The dashed line is normalized to the V_c corresponding to V_{DC} equal to 9 V. The lack of correlation between this line and the data points obtained experimentally, clearly demonstrates that the breakdown signal is a characteristic of the protoplasts and not a system artifact. It should be noted that these protoplasts were prepared from plants grown in February, 1979, using the same preparation as described before except for a 2% wt/vol PVP (polyvinyl pyrrolidone) addition to avoid damage of the cells during preparation. PVP probably suppresses the destruction of the membrane due to the presence of polyphenols which occur in plants grown in the winter season. A further change in the experimental conditions was the use of 700 instead of 600 mM mannitol in the resuspension and measuring media

of breakdown seen in the experiments described in Table 1.

It should be noted that during any set of experiments, approximately one half are of pulse shapes without ramp, these being interspersed with ramp runs. When consistent irregularities in the pulse shape were observed, the experiment could be terminated until the problem (e.g., partial orifice blocking or incorrect flow rate) was corrected.

If the breakdown observed results purely from the system then changing the DC voltage applied across the orifice will have no effect upon the ramp signal, or to put it another way, the calculated critical membrane breakdown voltage will apparently become DC voltage dependent. In an experiment in which V_{DC} was varied from 2 to 12 V whilst keeping the same voltage ramp of 20 V over 70 μsec, the value of V_c was shown not to vary (Fig. 7). Also shown in Fig. 7 (dashed line) is the expected variation of V_c with V_{DC} under the assumption that the breakdown is a system artifact. From the lack of correlation between this dashed line and the line through the data points, it is obvious that the breakdown measured is a characteristic of the protoplasts and not a system artifact.

Finally, when the suction pressure on the orifices is a little high, or when a particle is detected late in its transit through the orifice, the particle will leave the orifice before the first experiment is over. In Fig. 8*a* two curves are shown: the flatter one is just a Latex particle of 14 μm diameter with an arrow indicating the departure time of the particle from the orifice; no ramp has been applied. The other curve is the result of multiplying an appropriate ramp function with the curve described above. This therefore is what should be seen if a particle leaves the orifice when the ramp is being applied during an experiment. Just such a curve is seen in Fig. 8*b* for a 18.5 μm diameter Latex particle. It is obvious that this event could not possibly be confused with that of breakdown as described for protoplasts.

Discussion

The data presented here on guard cell protoplasts isolated from leaves of *Vicia faba* demonstrate that the new technique is capable of determining from only a single cell, the volume, electrical breakdown of the cell membrane, and the underestimation of the volume after breakdown which is related to both

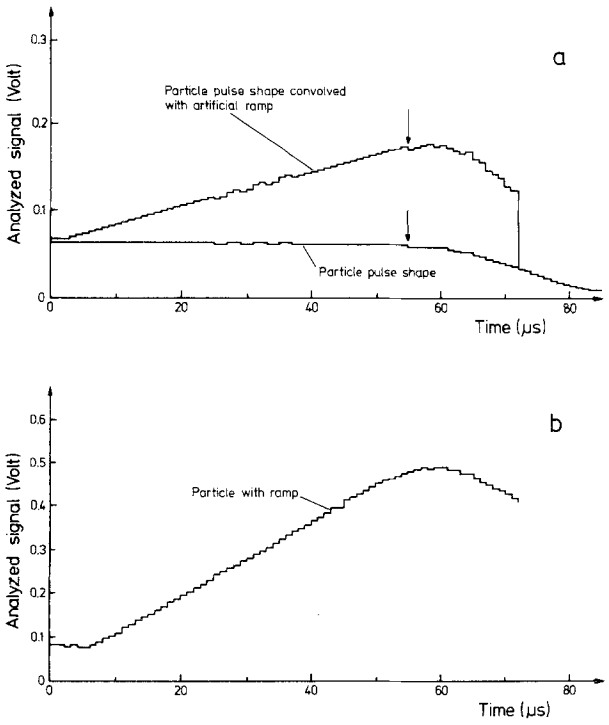

Fig. 8. Effect on the ramp signal of a particle leaving the orifice before the ramp is finished. A Latex particle of 14 µm in diameter leaves the orifice 55 µsec after size detection, giving the observed pulse shape (*a*). This pulse is then multiplied with a 70 µsec long ramp function to demonstrate the characteristic curvature of the ramp signal (*a*) when the particle leaves too soon. The similarity of the ramp signal seen in *b* (for Latex particle of 18 µm in diameter), this time with the voltage ramp applied across the orifices, to that in *a* indicates that the particle in *b* left the orifice before the ramp was terminated

the internal and reduced membrane conductivity relative to the external conductivity of the sheath flow [17, 43]. This represents considerable progress when compared to the technique using the hydrodynamically focusing Coulter Counter, especially for the particles used here which are contaminated with debris of clustered chloroplasts, residual epidermis protoplasts, cell walls, destroyed guard cell protoplasts from the preparation procedure and are not normally distributed. The technique also requires very few cells.

Artifacts introduced by the detection and analysis system can be excluded or distinguished from cellular phenomenon. As discussed earlier, the temperature increase in the orifices is very small and therefore plays no role in the observed breakdown. Although there were signals in which breakdown was not observed, these can mostly, however, be attributed to either debris or clumped chloroplasts (this is discussed further below). In addition to the control experiments made with both protoplasts and Latex particles, recent measurements on rat brain tumor cells support the results here. It should be noted that rat brain tumor cells exhibit a much sharper change in the slope of the ramp signal after breakdown as compared with that observed in protoplasts (*unpublished data*).

So far in the calculation of the breakdown voltage, V_c, it has been implicitly assumed that the cells are spherical and noncompartmented. When these conditions are not fulfilled one may expect to observe deviations from a V_c of 1 V and an effect upon R_S. However, the protoplasts investigated here are certainly compartmented. Light micrographs (Fig. 9) indicate

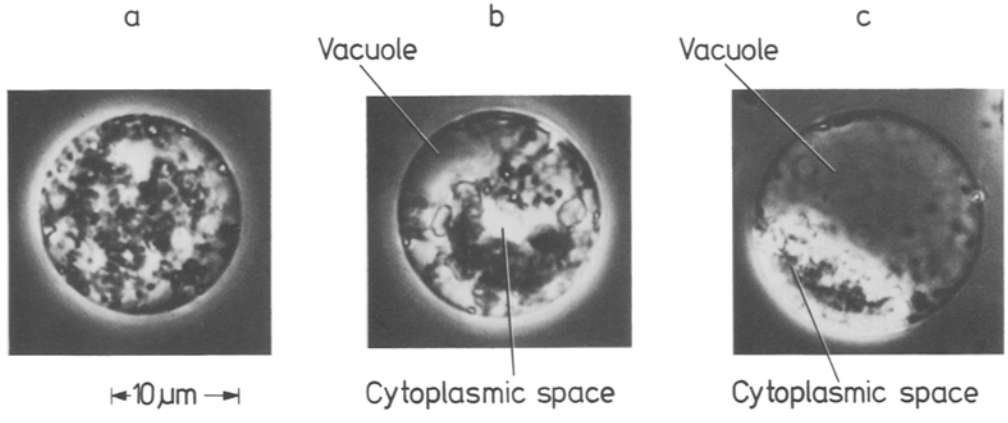

Fig. 9. Phase contrast light micrographs of guard cell protoplasts from *Vicia faba* showing various stages of vacuole differentiation. The protoplasts are from one preparation. Note that in *a* the cytoplasm is distributed homogeneously, no vacuole being visible, and that in *b* the vacuole although small is visible, whilst in *c* the vacuole occupies approximately 80% of the total volume. These morphological variations and different orientations of protoplasts within the orifice are reflected in the differences of the volume underestimation after breakdown (*see* text)

that the protoplasts consist of membranes in series with each other (plasmalemma and tonoplast) with the vacuolar dimensions differing from cell to cell depending upon size, age, and the physiological state of the stomata. In addition, the nucleus and the plastids containing considerable but variable amounts of starch occupy a large part of the protoplast volume. If their dimensions are small the vacuolar and plastid compartments would not contribute very much to the signal of the cell when breakdown of the plasmalemma has occurred. According to Eq. (5) the external field strength required for taking the membrane potential to its critical breakdown value is inversely proportional to the radius. Thus, provided that the breakdown voltage of the subcellular membranes is of the same order as that for the plasmalemma, only the plasmalemma would break through in response to the external field. Consequently, the degree of underestimation expressed by $(1-R_s)$ would predominantly depend upon the size and conductivity of the cytoplasmic space, and thus on the number of osmotically active ions in the cytoplasm in addition to the reduced membrane conductivity. However, for internal compartments of larger dimensions one could expect, particularly for the highly conducting tonoplast, a significant effect upon the breakdown signal depending upon the orientation of the compartment within the cell relative to the externally applied field. Either the value for the relative size after breakdown, R_S, would be close to 1 because the tonoplast shields most of the internal volume, or the tonoplast would have to break down in addition to the plasmalemma leading to a lower R_S value due to the high conductance state of the vacuolar space. Thus, it is immediately obvious that R_S should vary considerably in the experiments, which was indeed demonstrated.

A correlation of the R_S value determined for a single cell with the geometrical dimensions of the subcellular compartments of a given cell is required for future experiments. Knowledge of the relationship between the R_S values and cell compartments would considerably extend the application of such breakdown experiments particularly when applied to different states of cell development or to different environmental conditions (water and salt stress, CO_2 supply, etc.).

Associated with the observed variation in R_S, one should expect to occasionally see fluctuations in the breakdown voltage, given the above explanation for R_S variability. The breakdown voltage of about 1 V observed in all experiments is very much the same as that found for the membrane of animal cells (erythrocytes [38] and lymphocytes [41] and bacteria (*Escherichia coli* B 163 [39, 43]) which are surrounded by a single membrane. If two membranes are arranged in series and close together at the point of breakdown a doubling of the breakdown voltage would be expected. It is unlikely, however, that this condition would often be fulfilled for the protoplasts because of different orientations of the vacuole within the cell despite the occurrence of large vacuoles (*see* Fig. 9). There are particles in the experiments reported here for which no breakdown is observed over the limited applied external field. These may either reflect cases in which the breakdown voltage is doubled but is therefore out of range or, as previously stated and more likely, reflect the presence of debris or clumped chloroplasts.

An alternative explanation for the relatively small variation in the breakdown voltage for protoplasts may be that the tonoplast is already a highly conducting membrane. Thus, if the charging current is too low an insufficient charging of the membrane would occur. A breakdown voltage of 1 V has also been found using a hydrodynamically focusing Coulter Counter for both etioplasts and chloroplasts [24] which are known to be surrounded by two membrane envelopes. The outer envelope membrane though is very conducting [13, 14] and would therefore not contribute very much to the measurement. Recently, experiments in which the tonoplast of perfused cells of *Chara corallina* were removed demonstrated that the resistance to water flow of the plasmalemma is indeed much higher than that of the tonoplast [19]. However, a breakdown voltage of 2.2 V has been observed in the multicompartmental cells of *Ochromonas malhamensis* [40, *see also* 24]. On the other hand, *Valonia utricularis* and *V. ventricosa* show a breakdown voltage of 0.9 V (17 °C) [6, 37] even though two membranes should exhibit breakdown as the vacuole occupies 95% of the cell volume.

In the case of a breakdown of two membranes, the breakdown voltage of the single membrane would be of the order of 0.45 V, assuming that both membranes exhibit the same breakdown voltage. This value is close to that reported for *Fucus erratus* (0.5 to 0.58 V, pulse length 1 to 1000 μsec, seawater [9]). *Fucus erratus* is surrounded by a single membrane, only. Very recent experiments on bilayers and *V. utricularis* using the charge pulse technique ([1], R. Benz & U. Zimmermann, *in preparation*) revealed that the breakdown voltage is pulse-length dependent. The breakdown voltage of a bilayer made up of oxidized cholesterol and bathed in a 1 M KCl solution increased from about 0.5 V at a pulse length of 5 μsec to about 1 V and more for pulse lengths of 0.8 μsec. In a comparable range of pulse lengths, the similar result was found for *V. utricularis* bathed in seawater. Thus, it seems possible that the differences in the absolute value of the breakdown voltage for a single

membrane may be traced back to a pulse-length dependence which may vary from one species to the other one.

It should be finally mentioned that in terms of the electro-mechanical model a breakdown voltage of 1 V means that the compressive elastic modulus transverse to the membrane of guard cell protoplasts is similar to that of other osmoregulating algal cells [7, 34, 35, 44]. Thus protoplasts should preferably osmoregulate their internal osmolarity in response to the external salinity.

With further improvements in the technique, it will also be possible to extend the measurements presented in this paper to smaller cells and also to follow rapid volume changes in conjunction with the breakdown measurements. It should then be possible to both follow and better understand the osmoregulation processes associated with microscopic plant cells.

We are indebted to Drs. Brocke and Holzapfel, KFA Jülich, to Dr. Kachel, MPI München, and to Prof. Dr. Ziegler, TU München, for stimulating discussions of the manuscript and the equipment. We would also like to thank Ing. (grad.) H. Koch, KFA Jülich, for expert technical assistance, and Mr. Mommertz, KFA Jülich, for workshop skills.

This work was supported partly by a grant to U.Z. from the SFB 160, and partly by a grant to U.Z. from the BMFT, No. BCT 112.

References

1. Benz, R., Beckers, F., Zimmermann, U. 1979. Reversible electrical breakdown of lipid bilayer membranes: A charge-pulse relaxation study. *J. Membrane Biol.* **48**:181
2. Carstensen, E.L. 1967. Passive electrical properties of microorganisms: II. Resistance of the bacterial membrane. *Biophys. J.* **7**:493
3. Carstensen, E.L., Cox, H.A., Mercer, W.B., Natale, L.A. 1965. Passive electrical properties of microorganisms: I. Conductivity of *Escherichia coli* and *Micrococcus lysodeikticus*. *Biophys. J.* **5**:289
4. Carstensen, E.L., Marquis, R.E. 1968. Passive electrical properties of microorganisms: III. Conductivity of isolated bacterial cell walls. *Biophys. J.* **8**:536
5. Coster, H.G.L., Steudle, E., Zimmermann, U. 1976. Turgor pressure sensing mechanism. *Plant Physiol.* **58**:636
6. Coster, H.G.L., Zimmermann, U. 1975. The mechanism of electrical breakdown in the membranes of *Valonia utricularis*. *J. Membrane Biol.* **22**:73
7. Coster, H.G.L., Zimmermann, U. 1976. Transduction of cell turgor pressure by cell membrane compression. *Z. Naturforsch.* **31c**:461
8. Cowen, I.R., Farquhar, G.D. 1977. Stomatal function in relation to leaf metabolism and environment. *In:* D. Jennings, editor. Proc. Symp. Exp. Biol. 31 Integration of Activity in the Higher Plant. pp. 471–505. Cambridge University Press, Cambridge
9. Gauger, B., Bentrup, F.W. 1979. A study of dielectric membrane breakdown in the *Fucus* egg. *J. Membrane Biol.* **48**:249
10. Gregg, E.C., Steidley, K.D. 1965. Electrical counting and sizing of mammalian cells in suspension. *Biophys. J.* **5**:393
11. Grover, N.B., Naaman, J., Ben-Sasson, S., Doljanski, F. 1969. Electrical sizing of particles in suspension: I. Theory. *Biophys. J.* **9**:1389
12. Grover, N.B., Naaman, J., Ben-Sasson, S., Doljanski, F., Nadov, B. 1969. Electrical sizing of particles in suspensions: II. Experiments with rigid spheres. *Biophys. J.* **9**:1415
13. Hampp, R. 1978. Kinetics of membrane transport during chloroplast development. *Plant Physiol.* **62**:735
14. Heldt, H.W., Sauer, F. 1971. The inner membrane of the chloroplast envelope as the site of specific metabolite transport. *Biochim. Biophys. Acta* **234**:83
15. Hsiao, T.C. 1976. Stomatal ion transport. *In:* Transport in Plants. II, Part B: Tissues and Organs. U. Lüttge and M.G. Pitman, editors. pp. 195–221 Springer-Verlag, Berlin–Heidelberg–New York
16. Hurley, J. 1970. Sizing particles with a Coulter Counter. *Biophys. J.* **10**:74
17. Jeltsch, E., Zimmermann, U. 1979. Particles in a homogeneous electric field: A model for the electrical breakdown of living cells in a Coulter Counter. *Bioelectrochem. Bioenerg. (in press)*
18. Kachel, V. 1976. Basic principles of electrical sizing of cells and particles and their realization in the new instrument "Metricell". *J. Histochem. Cytochem.* **24**:211
19. Kiyosawa, K., Tazawa, M. 1977. Hydraulic conductivity of tonoplast-free *Chara* cells. *J. Membrane Biol.* **37**:157
20. Kubitschek, H.E. 1960. Electronic measurement of particle size. *Research (London)* **13**:128
21. Lösch, R. 1977. Responses of stomata to environmental factors–experiments with isolated epidermal strips of *Polypodium vulgare*: I. Temperature and humidity. *Oecologia (Berlin)* **29**:85
22. Lösch, R., Schenk, B. 1978. Humidity responses of stomata and the potassium content of guard cells. *J. Exp. Bot.* **29**:781
23. Meidner, H., Mansfield, T.A. 1968. Physiology of stomata. McGraw-Hill, London
24. Pilwat, G., Hampp, R., Zimmermann, U. 1979. Electrical field effects induced in membranes of developing chloroplasts. *Planta (in press)*
25. Pilwat, G., Zimmermann, U., Riemann, F. 1975. Dielectric breakdown measurements of human and bovine erythrocyte membranes using benzyl alcohol as a probe molecule. *Biochim. Biophys. Acta* **406**:424
26. Raschke, K. 1975. Stomatal action. *Annu. Rev. Plant Physiol.* **26**:309
27. Raschke, K. 1977. The stomatal turgor mechanism and its responses to CO_2 and abscisic acid: Observations and a hypothesis. *In:* Regulation of Cell Membrane Activities in Plants. E. Marrè and O. Ciferri, editors. pp. 173–183. North Holland, Amsterdam
28. Raschke, K. 1979. Movements of stomata. *In*: Physiology of Movements Encyclopedia of Plant Physiology. W. Haupt and M.E. Feinleib, editors. Vol. 7, pp. 383–441. Springer-Verlag, Heidelberg
29. Schnabl, H. 1978. The effect of Cl^- upon the sensitivity of starch-containing and starch-deficient stomata and guard cell protoplasts towards potassium ions, fusicoccin and abscisic acid. *Planta* **144**:95
30. Schnabl, H., Bornman, Ch.H., Ziegler, H. 1978. Studies on isolated starch containing (*Vicia faba*) and starch deficient (*Allium cepa*) guard cell protoplasts. *Planta* **143**:33
31. Schnabl, H., Ziegler, H. 1977. The mechanism of stomatal movement in *Allium cepa L. Planta* **136**:37
32. Schwan, H.P. 1957. Electrical properties of tissue and cell sus-

pensions. *In:* Advances in Biological and Medical Physics V. J.H. Lawrence and C.A. Tobias, editors. Academic Press, New York

33. Zeiger, E., Hepler, P.K. 1976. Production of guard cell protoplasts from onion and tobacco. *Plant Physiol.* **58:**492
34. Zimmermann, U. 1977. Cell turgor pressure regulation and turgor pressure-mediated transport processes. *In: Proc. Symp. Exp. Biol.* Vol. 31, pp. 117–154. Integration of Activity in the Higher Plant. D. Jennings, editor. Cambridge University Press, Cambridge
35. Zimmermann, U. 1978. Physics of turgor- and osmoregulation. *Ann. Rev. Plant Physiol.* **29:**121
36. Zimmermann, U., Beckers, F., Coster, H.G.L. 1977. The effect of pressure on the electrical breakdown in the membranes of *Valonia utricularis*. *Biochim. Biophys. Acta* **461:**399
37. Zimmermann, U., Beckers, F., Steudle, E. 1977. Turgor sensing in plant cells by the electro-mechanical properties of the membrane. *In:* Transmembrane Ion Exchange in Plants. M. Thellier, A. Monnier, M. Demarty, and J. Dainty, editors. pp. 155–165. CNRS, Paris
38. Zimmermann, U., Pilwat, G., Beckers, F., Riemann, F. 1976. Effects of external electric fields on cell membranes. *Bioelectrochem. Bioenerg.* **3:**58
39. Zimmermann, U., Pilwat, G., Riemann, F. 1974. Dielectric breakdown of cell membranes. *Biophys. J.* **14:**881
40. Zimmermann, U., Pilwat, G., Riemann, F. 1974. Dielectric breakdown in cell membranes. *In:* Membrane Transport in Plants. U. Zimmermann and J. Dainty, editors. pp. 146–153. Springer-Verlag, Heidelberg
41. Zimmermann, U., Pilwat, G., Vienken, J. 1979. Erythrocytes and lymphocytes as drug carrier systems: Techniques for entrapment of drugs in living cells. *In:* Recent Results in Cancer Research. G. Mathé, editor. Springer-Verlag, Berlin – Heidelberg – New York (*in press*)
42. Zimmermann, U., Riemann, F., Pilwat, G. 1976. Enzyme loading of electrically homogeneous human red blood cell ghosts prepared by dielectric breakdown. *Biochim. Biophys. Acta* **436:**460
43. Zimmermann, U., Schulz, J., Pilwat, G. 1973. Transcellular ion flow in *E. coli B* and electrical sizing of bacteria. *Biophys. J.* **13:**1005
44. Zimmermann, U., Steudle, E. 1978. Physical aspects of water relations of plant cells. *Adv. Bot. Res.* **6:**45

Received 7 May 1979; revised 17 September 1979